Table S1 (*this has been revised) – Table of new cores collected in the Mid-Barataria Diversion receiving basin highlighting core environment (marsh, bay, paleochannel), date of collection, location information, core length, core compaction, and core elevation extracted from USGS 2022 Topobathy dataset. See figures S1-S3 for core locations in GIS.

Site	Site Type	Borehole Number	Date collected	Latitude	Longitude	Elevation from USGS 2022 Topobathy (m rel to NAVD 88)	V1 Length (cm)	V1 Compaction (cm)	V2 Length (cm)	V2 Compaction (cm)
T1-1	water/bay	602292002	30-Apr-2022	29.64040614	-89.99618312	-0.12	339.5	92	414.5	118
T1-5	land/paleochannel (Bayou Barataria)	602292004	1-May-2022	29.6730736	-90.1018783	-0.32	n/a	n/a	n/a	n/a
T3-1	water/bay	602292003	30-Apr-2022	29.606687	-89.99412	-0.11	564.5	23	422	60
T3-1.5	paleochannel (Bayou Barataria)	602292009	4-May-2022	29.5609646	-90.01984	0.29	223	184	222	241
T3-2	paleochannel (Bayou Barataria)	602292007	3-May-2022	29.5667116	-90.0286674	0.35	250.75	275	311.5	186
T3-3	marsh	602292008	3-May-2022	29.5617945	-90.0473708	0.37	354.5	196	375.5	170
T4-1	paleochannel (Bayou Dupont)	602292006	2-May-2022	29.606355	-89.982878	0.24	375	187	204.5	342.5
T4-2	water/bay	602292010	5-May-2022	29.554925	-89.977402	-0.10	421.5	68	422.5	48
T5-1	water/bay	602292001	29-Apr-2022	29.619763	-89.966517	-0.23	268.5	35	285	37
T5-2	marsh	602292005	2-May-2022	29.59825816	-89.93722853	0.20	374	139	420	153
L2 - 2023	paleochannel	60239005	17-May-2023	29.56943	-89.9871		n/a	n/a	n/a	n/a

Table S2 (*this has been revised) – Table vertical accretion rates from core samples extracted during this project. See Table S1 and Figure S1 for core locations.

Core Name	Site type	^{137}Cs Peak depth (cm)	Avg ^{137}Cs VAR (cm/yr)	210Pb CIC depth interval (cm)	210Pb CIC VAR (cm/yr)
T1-1	Water/bay	n/a	n/a	40-70	0.50
T1-5	Paleochannel/restored marsh	n/a	n/a	n/a	n/a
T3-1	Water/bay	n/a	n/a	0-30	0.36
T3-1.5	Marsh/paleochannel	80	1.36	10 – 40 & 80-115	0.81 & 1.46
T3-2	Marsh/paleochannel	90	1.53	50-90	1.46
T3-3	Marsh	45* (very small peak)	0.76*	15-40	0.49
T4-1	Marsh/paleochannel	70	1.19	14 – 40 & 50-70	0.81 & 1.17
T4-2	Water/bay	n/a	n/a	30-60	0.85
T5-1	Water/bay	n/a	n/a	25-60 & 85-105	0.73 & 0.73
T5-2	Marsh	70	1.19	40-80	1.16

Table S3 – Table of radiocarbon ages processed at Beta Analytic from core samples extracted during this project. Age is in years BP (before 1950). See Table S1 and Figure S1 for core locations.

MGII = T5-1
MGIII = T1-1
MGIV = T3-1
MGV = T4-2
MGVI = T4-1
MGVII = T3-2
MGVIII = T5-2

Sample Name	Depth (m)	Mean 14C age (BP)	Material
MGII-4	0.05-0.07	200 ± 11	a. 1 charcoal frag. b. 4 charcoal frag
MGII-2	0.48-0.51	1003 ± 11	a. 2 charcoal frag. b. 2 charcoal frag.
MGII-3	0.83-0.86	1350 ± 20	>10 charcoal frag.
MGII-1	1.12-1.15	1965 ± 20	>10 charcoal frag.
MGIII-3	0.1-0.12	230 ± 11	a. 1 charcoal frag. b. 4 charcoal frag
MGIII-4	0.61-0.64	893 ± 12	a. 1 charcoal frag. b. 6 Cyperaceae, *Schoenoplectus/Scirpus*
MGIII-2	1.38-1.39	1306 ± 12	a. 1 charcoal frag. b. 11 Cyperaceae, *Schoenoplectus/Scirpus*
MGIII-5	2.11-2.14	1883 ± 11	a. 8 Cyperaceae, *Schoenoplectus/Scirpus* b. 4 charcoal frag.
MGIII-1	2.46-2.49	2483 ± 14	a. >10 charcoal frag. b. 15 Alismataceae, *Sagittaria* sp.
MGIV-2	0.07-0.1	251 ± 22	a. 3 Cyperaceae, *Schoenoplectus/Scirpus* b. 5 charcoal frag.
MGIV-3	0.62-0.65	1253 ± 11	a. 1 charcoal frag. b. 2 charcoal frag.
MGIV-4	1.7-1.74	1950 ± 11	a. 8 cf. *Scirpus* achenes b. 4 charcoal frag.
MGIV-1	2.3-2.33	2543 ± 14	a. 1 charcoal frag. b. 11 cf. *Scirpus* achenes
MGIV-5	2.39-2.42	2555 ± 15	>10 charcoal frag.
MGV-1	0.28-0.30	1231 ± 12	a. 1 charcoal frag. c. 4 charcoal frag.
MGVI-1	1.63-1.69	915 ± 15	a. 7 charcoal frag.
MGVI-2	2.40-2.43	1410 ± 14	a. 4 charcoal frag. b. 1 *Scirpus* achenes, Cladium sp.
MGVI-6	2.57-2.60	1645 ± 45	4 charcoal frag.
MGVI-7	2.87-2.90	1980 ± 70	3 charcoal frag.
MGVI-3	3.79-3.82	2278 ± 14	a. 1 charcoal frag. b. 6 *Scirups* achenes, Cladium sp.
MGVI-4	4.14-4.17	2540 ± 20	a. 3 charcoal frag. b. 2 *Scirpus* achenes, Cladium sp.
MGVI-5	4.48-4.51	2655 ± 25	b. 4 charcoal frag.
MGVII-1	1.10-1.13	228 ± 11	a. 1 charcoal frag. c. 2 charcoal frag
MGVII-2	1.69-1.72	1105 ± 11	a. 2 charcoal frag. c. 3 charcoal frag
MGVIII-1	1.47-1.50	745 ± 31	a. 2 charcoal frag. b. 2 *Scirpus* achenes, Cladium sp.
MGVIII-2	2.07-2.10	998 ± 11	a. 1 charcoal frag. c. 2 charcoal frag
MGVIII-3	2.42-2.45	1232 ± 14	a. 1 charcoal frag. c. 4 charcoal frag

Table S4 (*this has been revised) – Table of preliminary Optically Stimulated Luminescence (OSL) ages from core samples extracted during this project. TBD = To Be Determined (analyses still underway). See Table S1 and Figure S1 for core locations.

(this was revised in December 2024)

Site	Borehole Number	Depth (cm)	Age (ka)
T1-1	602292002	290	TBD
T1-1	602292002	400	TBD
T1-5	602292004	140	TBD
T1-5	602292004	252	2.83 ± 0.14
T1-5	602292004	338	2.82 ± 0.47
T1-5	602292004	478	2.80 ± 0.14
T1-5	602292004	508	2.97 ± 0.19
T3-1	602292003	383	2.65 ± 0.14
T3-2	602292007	260	TBD
T3-2	602292007	280	TBD
T3-2	602292007	295	TBD
T4-1	602292006	308	2.12 ± 0.14
T4-2	602292010	163	1.29 ± 0.16
T4-2	602292010	288	2.03 ± 0.15
T4-2	602292010	402	2.87 ± 0.30
T5-1	602292001	233	2.40 ± 0.17
T5-1	602292001	263	2.49 ± 0.11
T5-2	602292005	310	TBD
T5-2	602292005	410	TBD

Site	Borehole Number	Depth (cm)	Age (ka)
T1-1	602292002	290	2.34 ± 0.13
T1-1	602292002	400	insufficient
T1-5	602292004	140	insufficient
T1-5	602292004	252	2.98 ± 0.15
T1-5	602292004	338	2.97 ± 0.49
T1-5	602292004	478	2.96 ± 0.15
T1-5	602292004	508	3.10 ± 0.20
T3-1	602292003	383	2.79 ± 0.15
T3-2	602292007	260	1.78 ± 0.16
T3-2	602292007	280	1.69 ± 0.14
~~T3-2~~	~~602292007~~	~~295~~	~~TBD~~
T4-1	602292006	308	2.23 ± 0.15
T4-2	602292010	163	1.38 ± 0.17
T4-2	602292010	288	2.09 ± 0.16
T4-2	602292010	402	2.95 ± 0.31
T5-1	602292001	233	2.50 ± 0.17
T5-1	602292001	263	2.61 ± 0.12
T5-2	602292005	310	1.16 ± 0.10
T5-2	602292005	410	1.16 ± 0.12

Table S5 (this has been revised) – Table of average bulk density, water content, organic content, porosity, and median grain size from 2 m deep auger cores. See Table S1 and Figure S1 for core locations. See Piorkowski MS Thesis for explanation and interpretation.

Site type	Dry bulk density (g/cm^3)	Water content %	Organic Matter %	Porosity %	Median grain size (phi)
Marsh	0.08 ± 0.02	74 ± 0.01	45.9 ± 1.5	94 ± 1	6.3 ± 0.4
Bay	0.36 ± 0.24	35.3 ± 16	19 ± 15	81.5 ± 10	6.7 ± 0.7
Paleochannel	0.12 ± 0.05	64.4 ± 9.8	33 ± 15	91 ± 3.1	6.3 ± 0.4

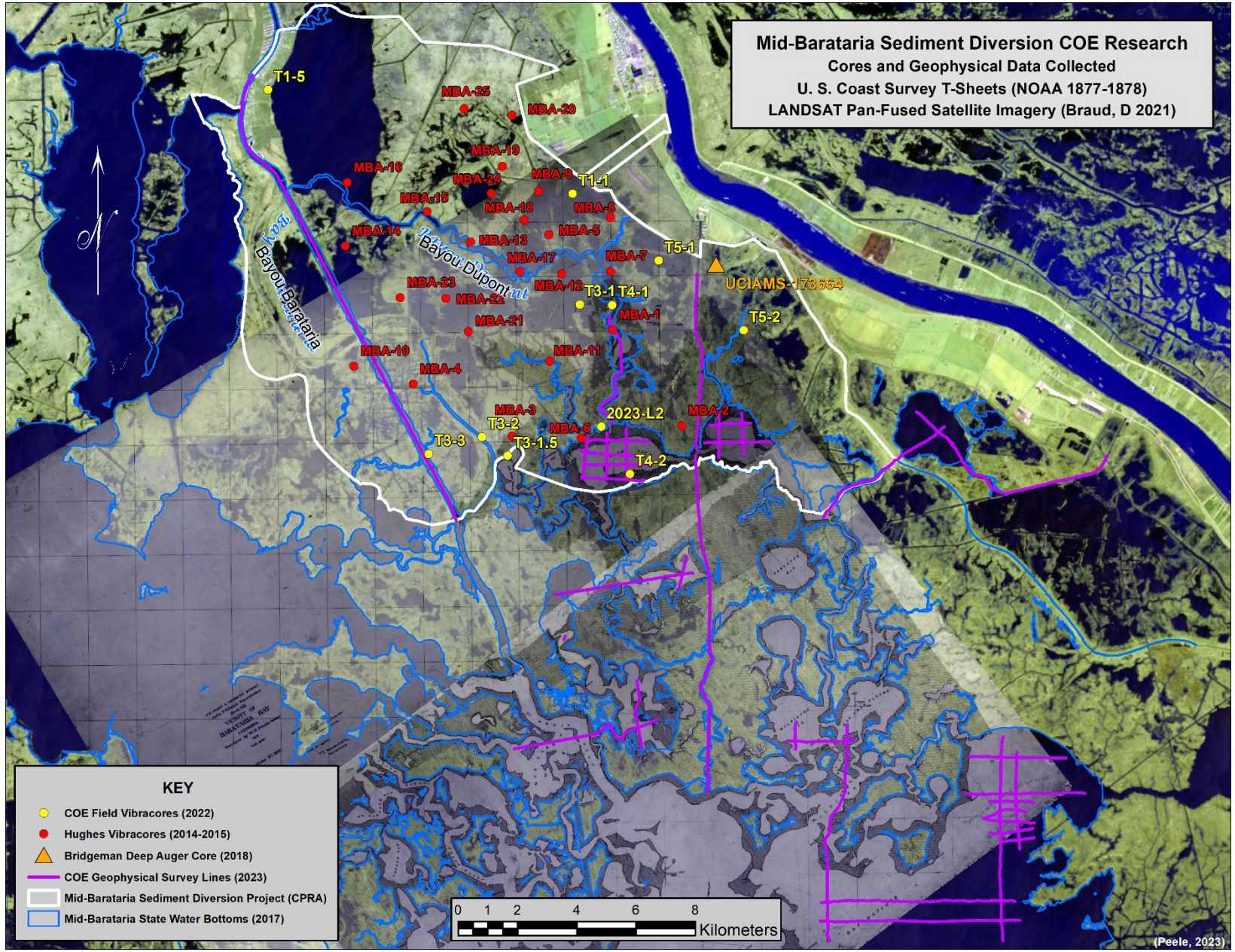

Figure S1– Summary of field data collected and reanalyzed in this COE project. The NOAA US Coast Survey T-sheets from 1877-1878 show the historical locations of Bayou Dupont and Bayou Barataria that dissect and form the western margin for the Mid-Barataria Sediment Diversion receiving basin, respectively. Approximately 170 km of geophysical lines were undertaken across the receiving basin, as well as to the south and southeast. Ten new auger cores coupled with vibracore samples were collected within the receiving basin in the following environments (marsh, bay, paleochannel) to achieve accurate lithology and chronology of deltaic deposits using isotopes ^{210}Pb and ^{137}Cs, ^{14}C, and Optically Stimulated Luminescence (OSL) over short to longer timescales (10^1-10^3 yr).

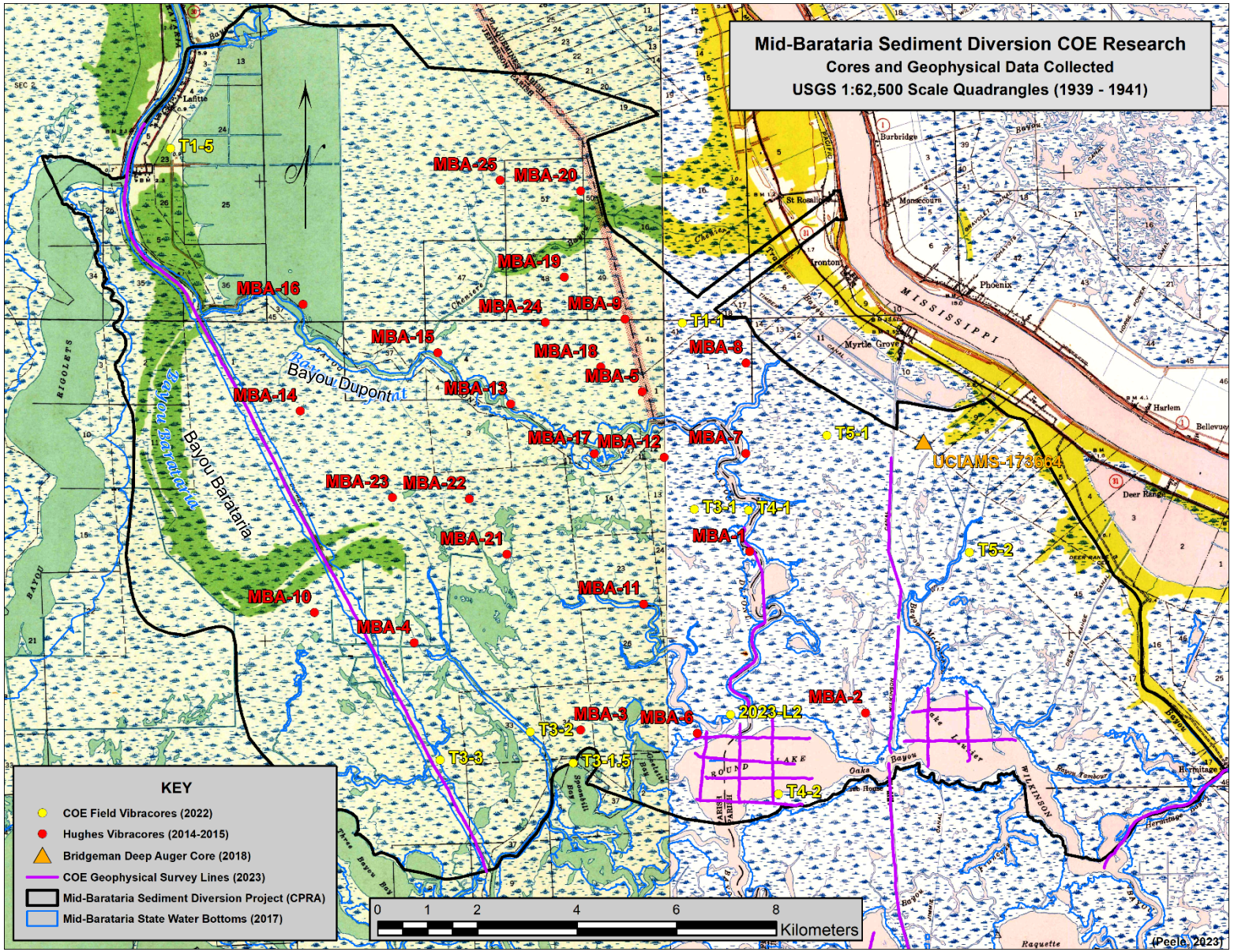

Figure S2 – This USGS 1:62,500 scale quadrangle maps from the 1940s (surveyed in 1939) shows the Mid-Barataria marsh with natural waterways such as Bayou Barataria and Bayou Dupont but few canals. These are the first large-scale topographical maps compiled from orthographic aerial photography depicting complete topographic coverage of the study area. The 2017 Louisiana State-Owned Water Bottoms are included for temporal reference. Any water bottoms not shown by blue line boundaries are privately owned.

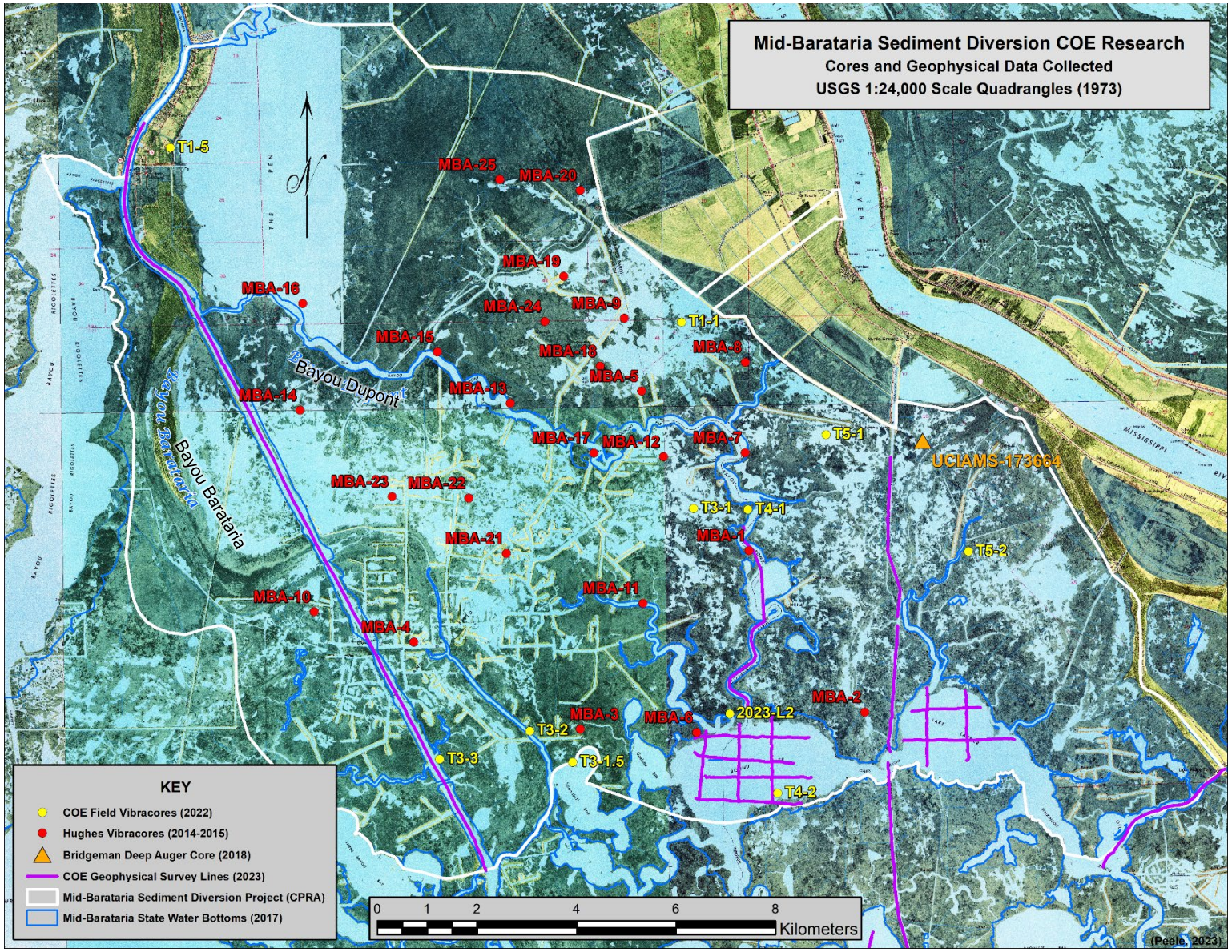

Figure S3 – This 1973 1:24,000 scale USGS quadrangle map shows many canals that have been constructed throughout the Mid-Barataria marsh. It also highlights how much marsh loss occurred between 1956 and 1973 (Couvillion et al., 2016). The 2017 Louisiana State-Owned Water Bottoms are included for temporal reference. Any water bottoms not shown by blue line boundaries are privately owned.

Figure S4 (*this has been revised) – Lithologic fence diagrams span NE to SW and NW to SE across the Mid-Barataria Diversion receiving basin in transect lines shown here. Deltaic lithology is shown in Fig S5 (A-F). See Piorkowski MS Thesis for explanation and interpretation of all fence diagrams.

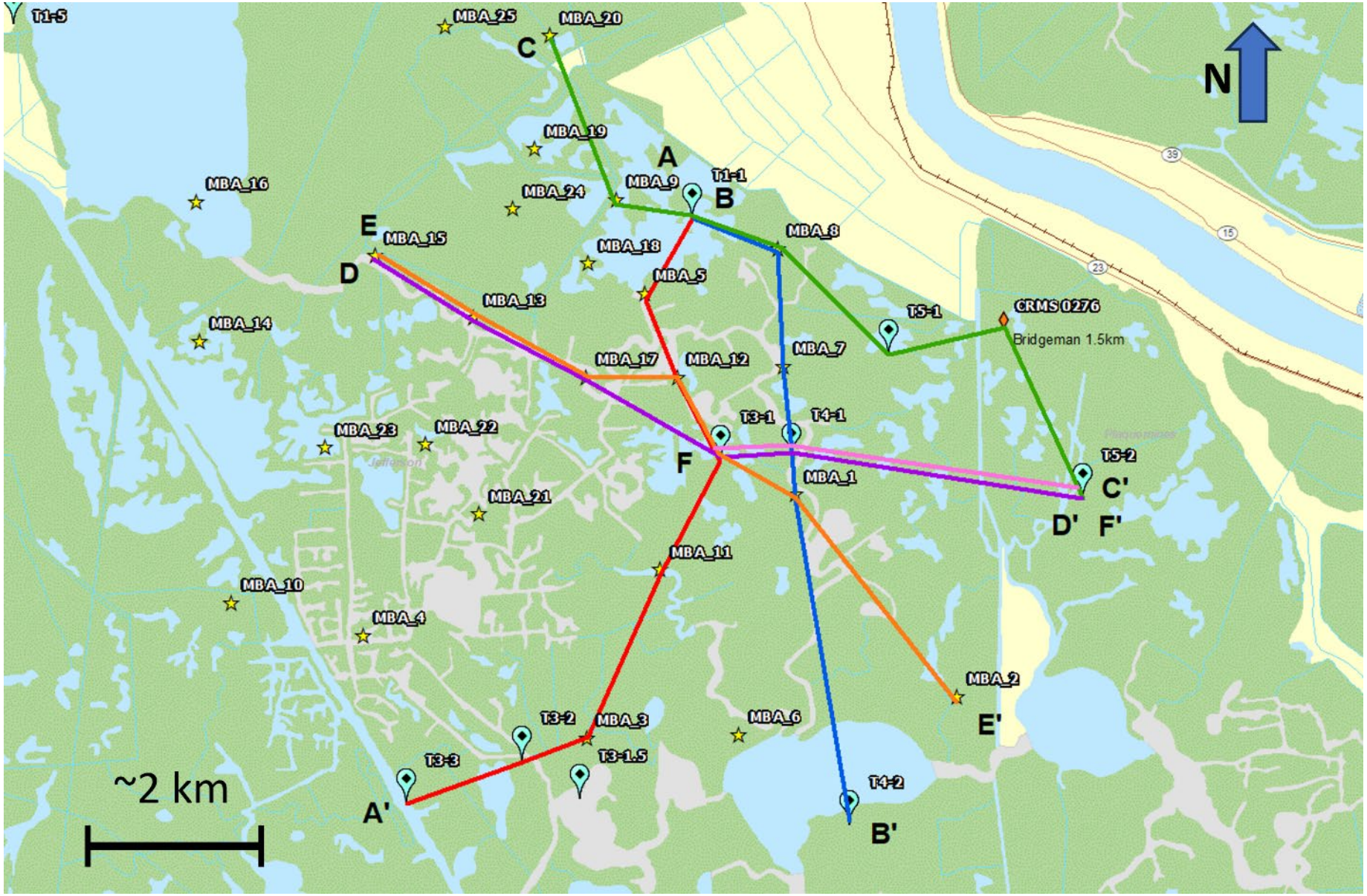

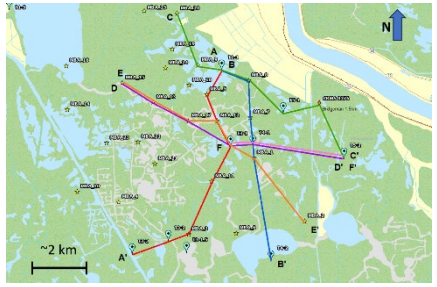

Figure S5 A (*this has been revised) – Deltaic lithology, as well as chronology results from this project using radioisotopes ^{210}Pb, ^{137}Cs, ^{14}C, and Optically Stimulated Luminescence (OSL). See Piorkowski MS Thesis for explanation and interpretation of all fence diagrams, though ages have been revised.

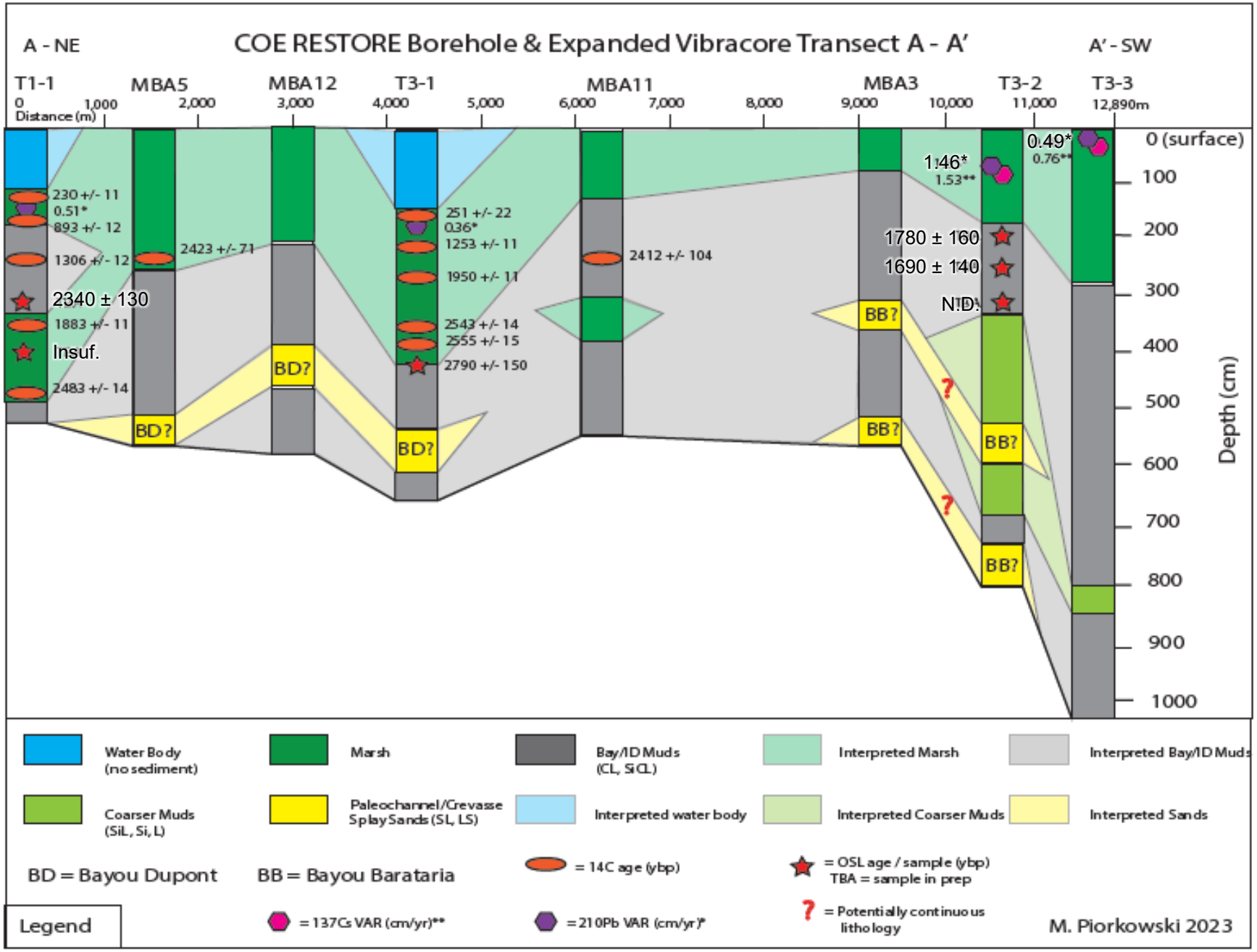

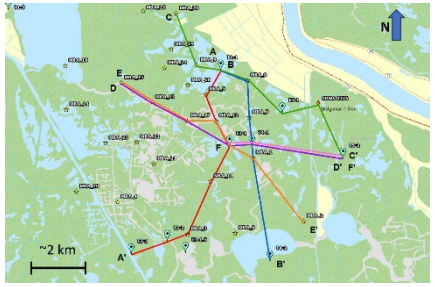

Figure S5 B (*this has been revised) –Deltaic lithology, as well as chronology results from this project using radioisotopes ^{210}Pb, ^{137}Cs, ^{14}C, and Optically Stimulated Luminescence (OSL). See Piorkowski MS Thesis for explanation and interpretation of all fence diagrams, though ages have been revised.

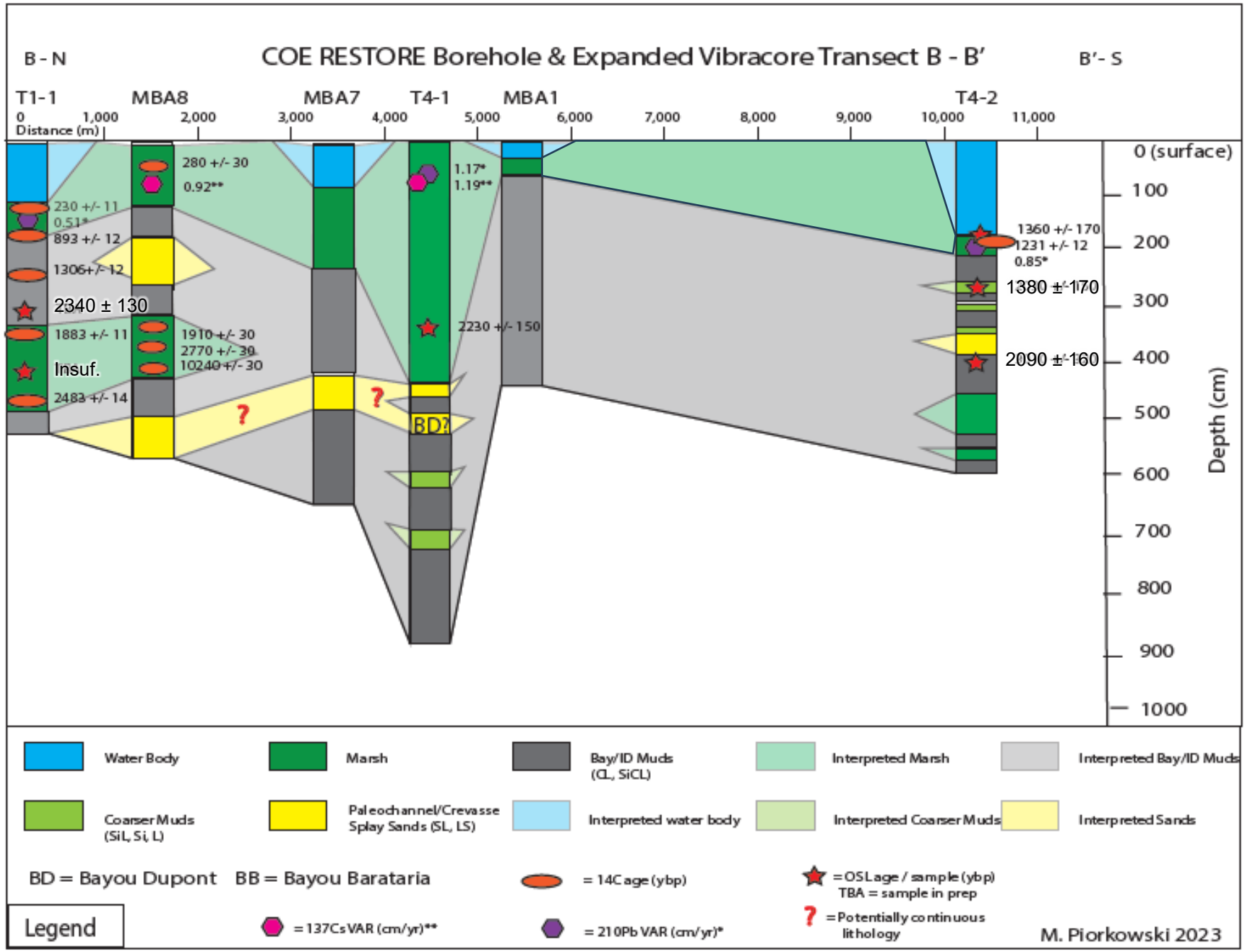

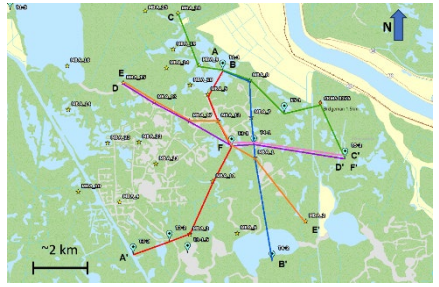

Figure S5 C (*this has been revised) –Deltaic lithology, as well as chronology results from this project using radioisotopes ^{210}Pb, ^{137}Cs, ^{14}C, and Optically Stimulated Luminescence (OSL). See Piorkowski MS Thesis for explanation and interpretation of all fence diagrams, though ages have been revised.

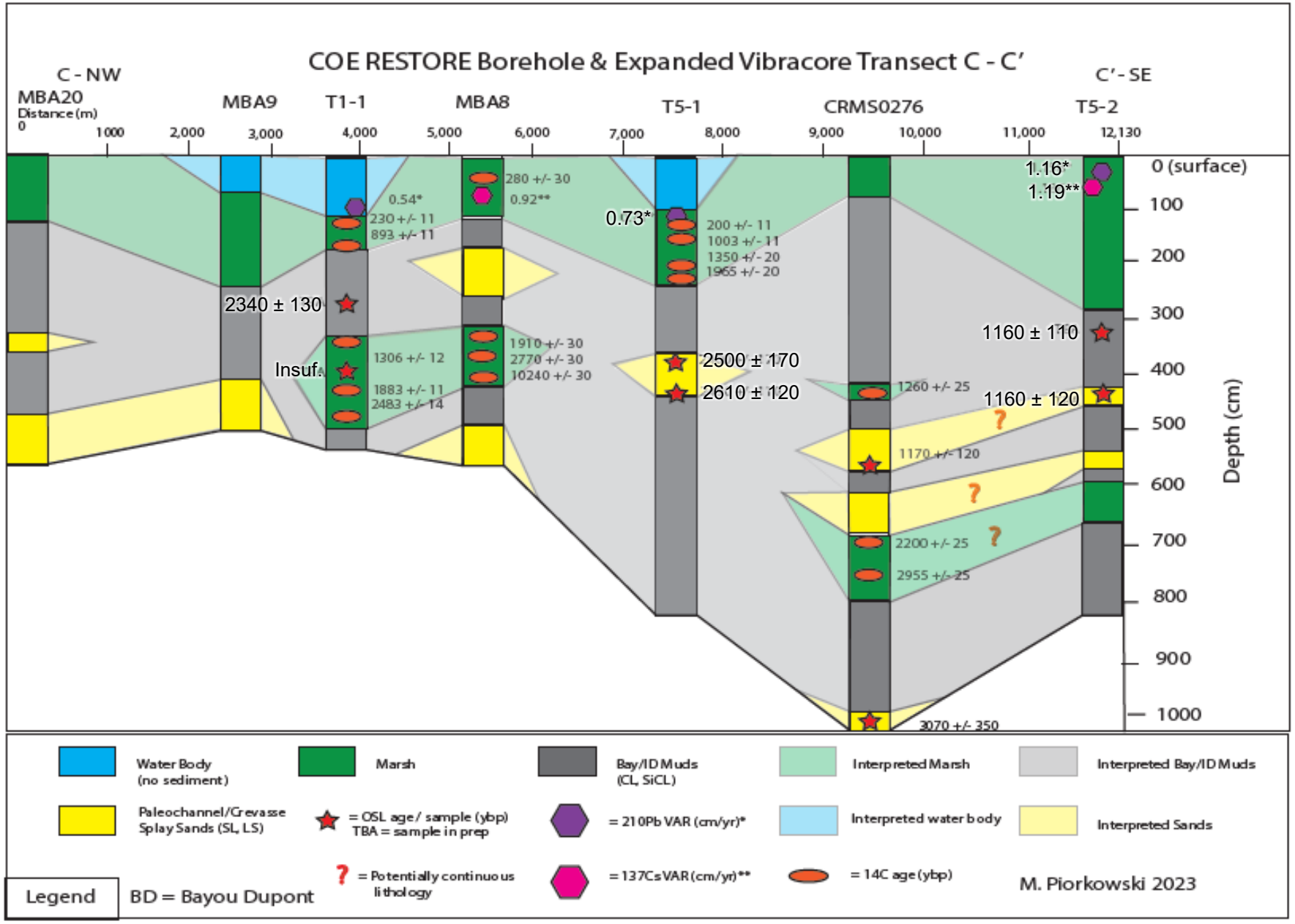

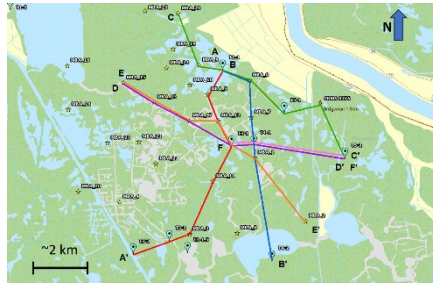

Figure S5 D (*this has been revised) –Deltaic lithology, as well as chronology results from this project using radioisotopes ^{210}Pb, ^{137}Cs, ^{14}C, and Optically Stimulated Luminescence (OSL). See Piorkowski MS Thesis for explanation and interpretation of all fence diagrams, though ages have been revised.

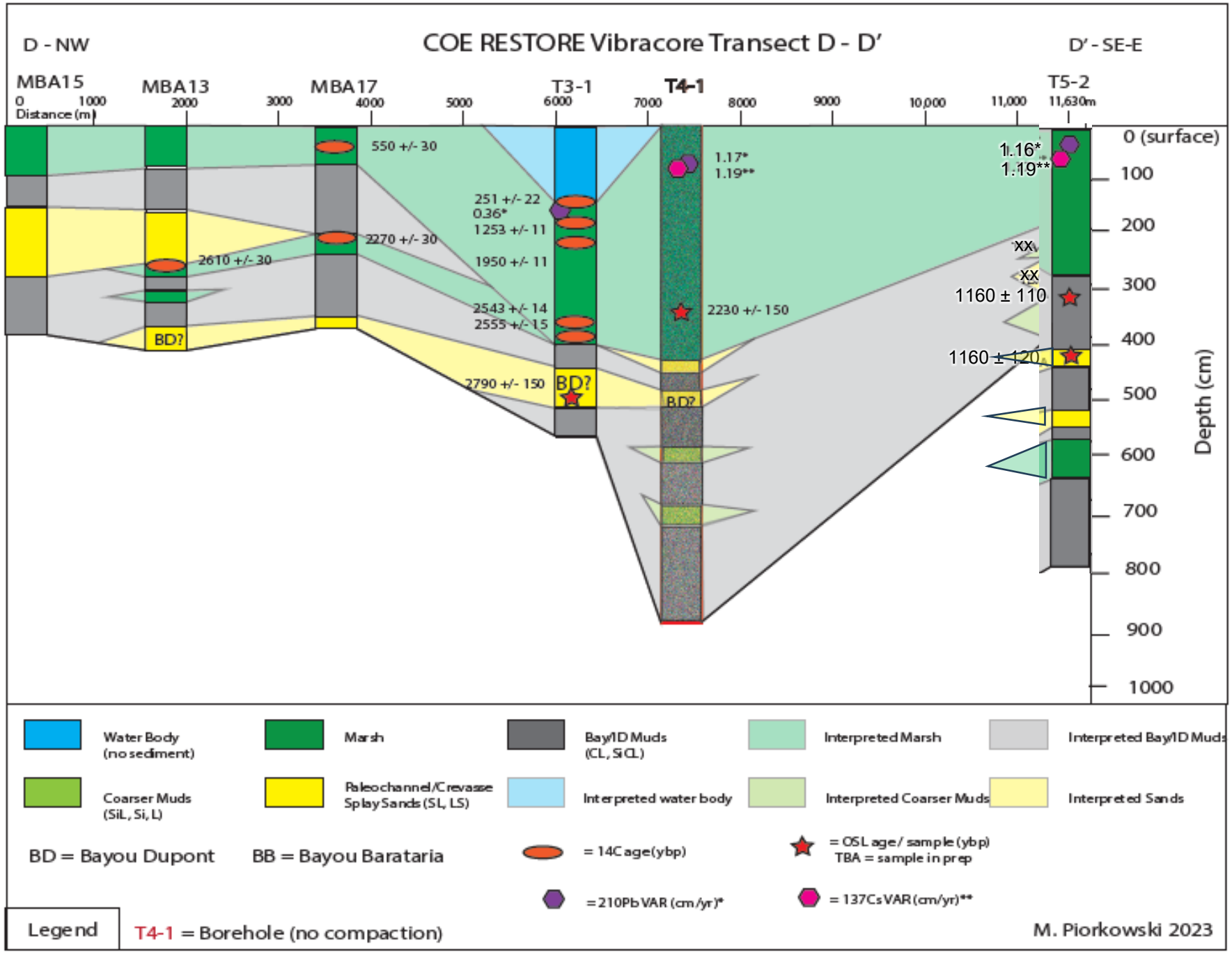

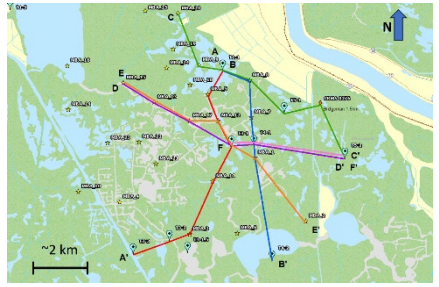

Figure S5 E (*this has been revised) –Deltaic lithology, as well as chronology results from this project using radioisotopes ^{210}Pb, ^{137}Cs, ^{14}C, and Optically Stimulated Luminescence (OSL). See Piorkowski MS Thesis for explanation and interpretation of all fence diagrams, though ages have been revised.

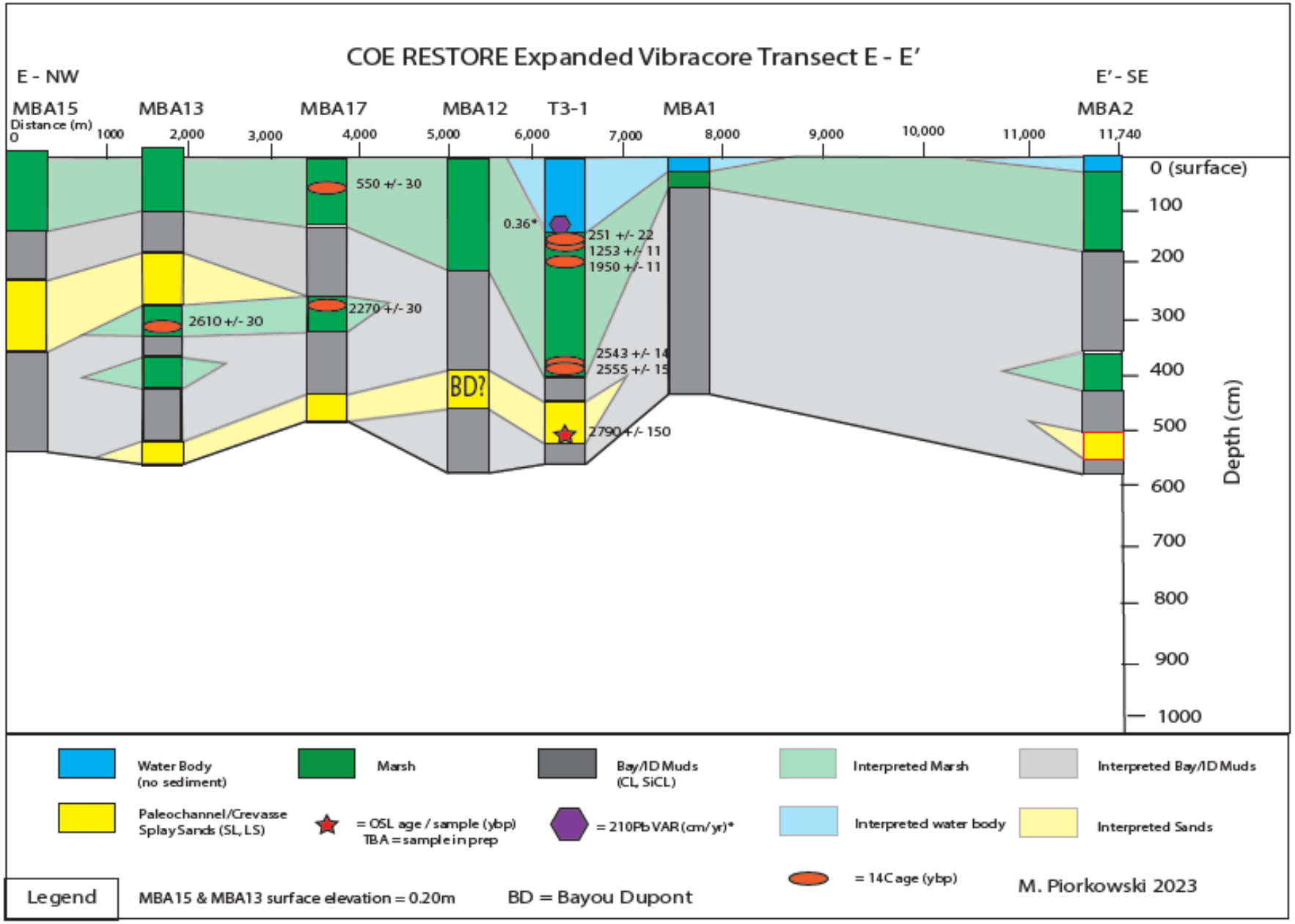

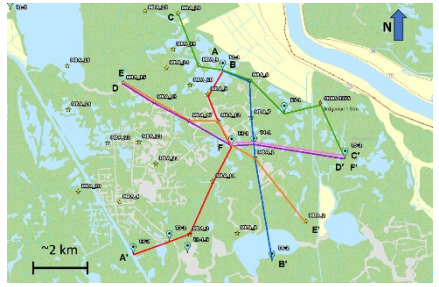

Figure S5 F (*this has been revised) –Deltaic lithology, as well as chronology results from this project using radioisotopes ^{210}Pb, ^{137}Cs, ^{14}C, and Optically Stimulated Luminescence (OSL). See Piorkowski MS Thesis for explanation and interpretation of all fence diagrams, though ages have been revised.

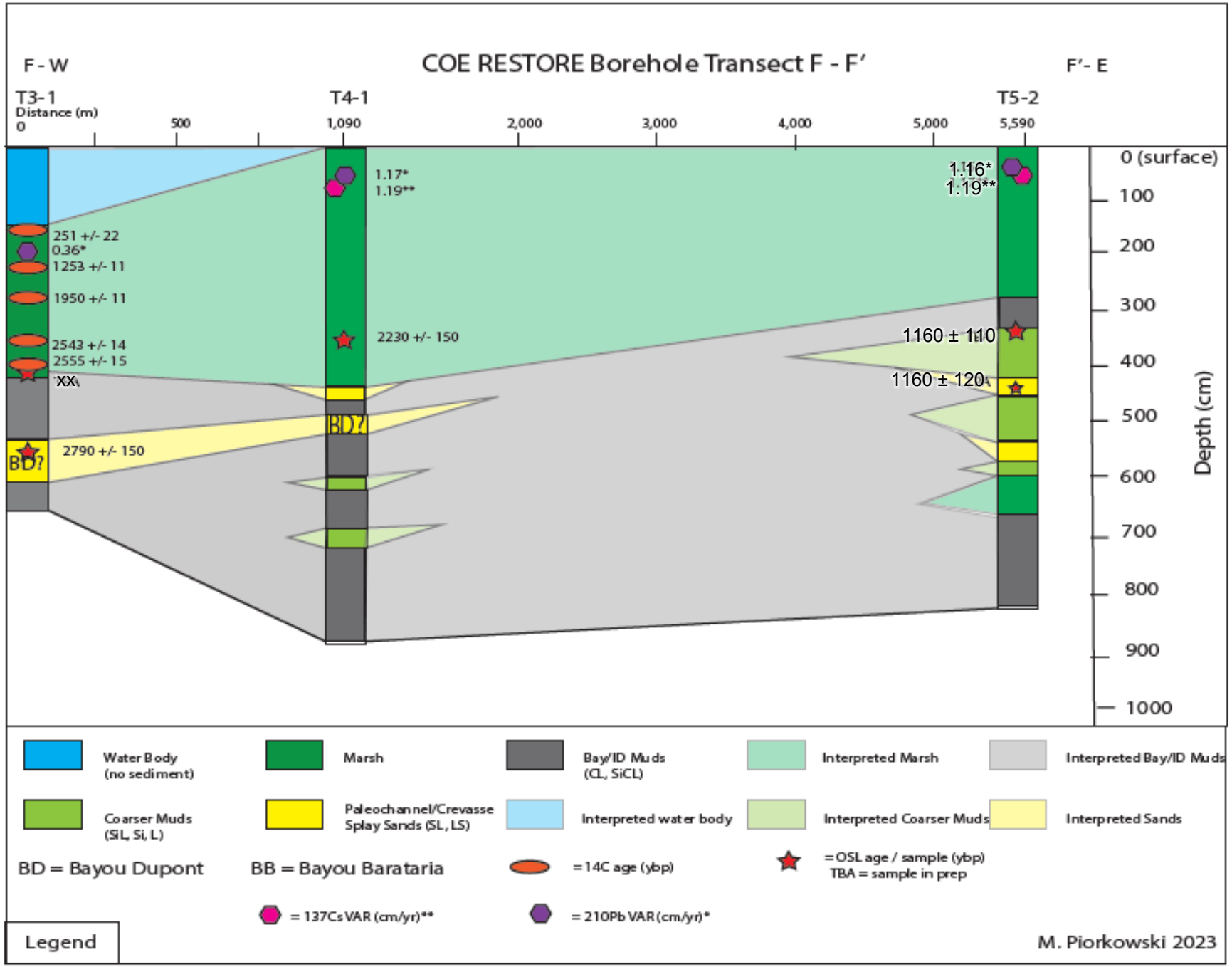

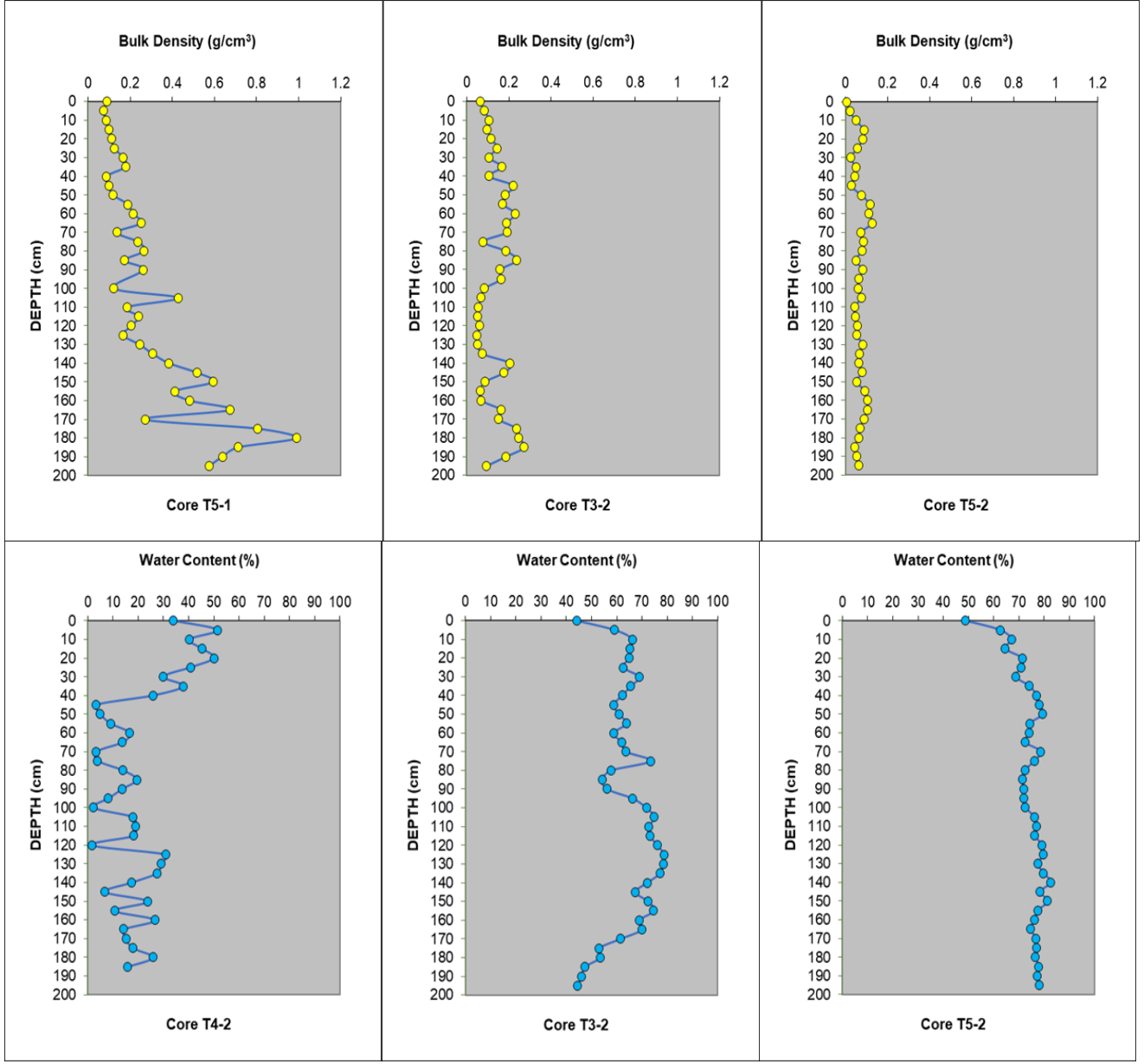

Figure S6 – Bulk density (top) and water content (bottom) for the upper 2 m of cores for representative bay (left), paleochannel (middle), and marsh (right) environments.

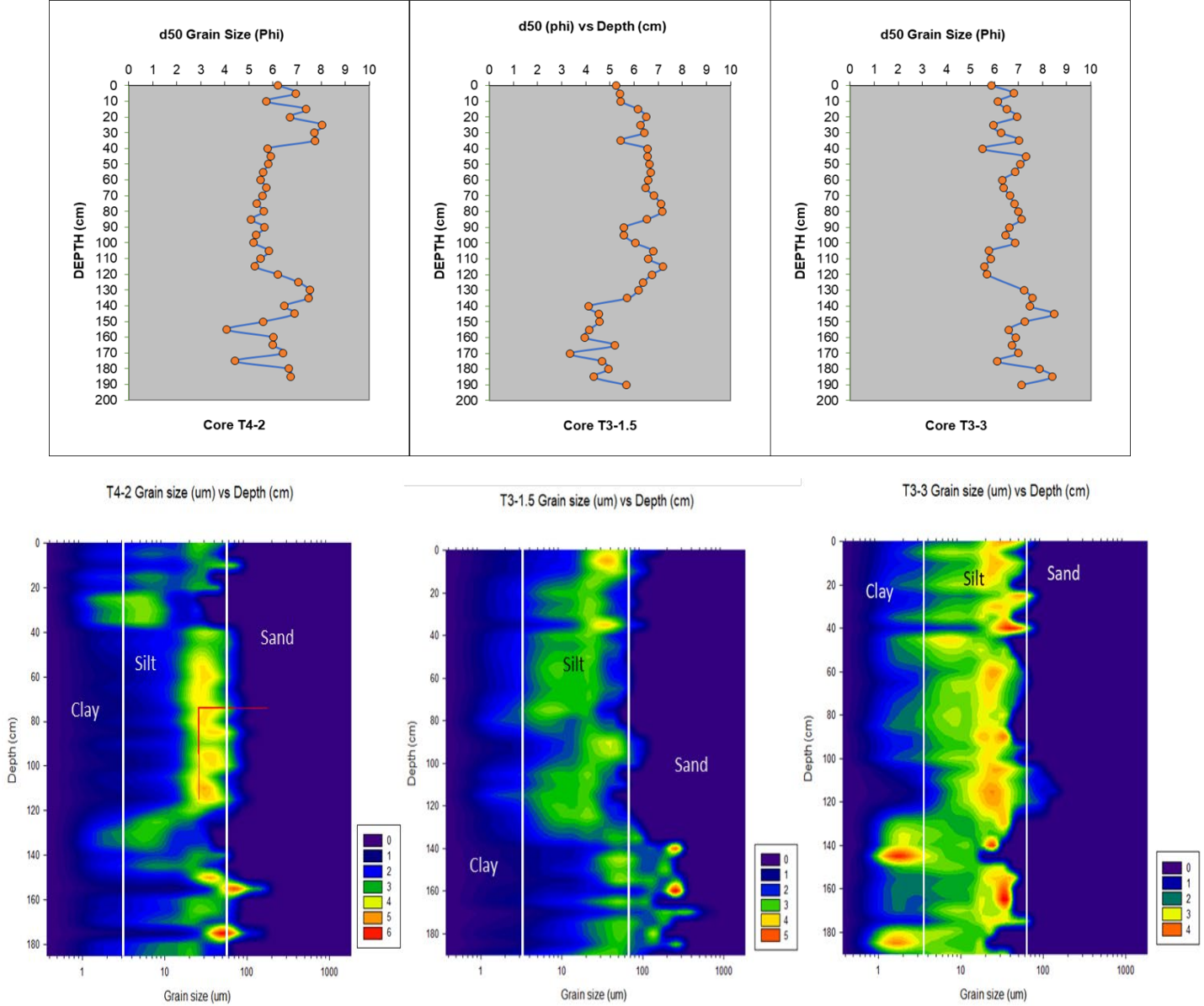

Figure S7 – Median D50 grain size in phi (top) and volume frequency grain size in microns (bottom) for the upper 2 m of cores for representative bay (left), paleochannel (middle), and marsh (right) environments.

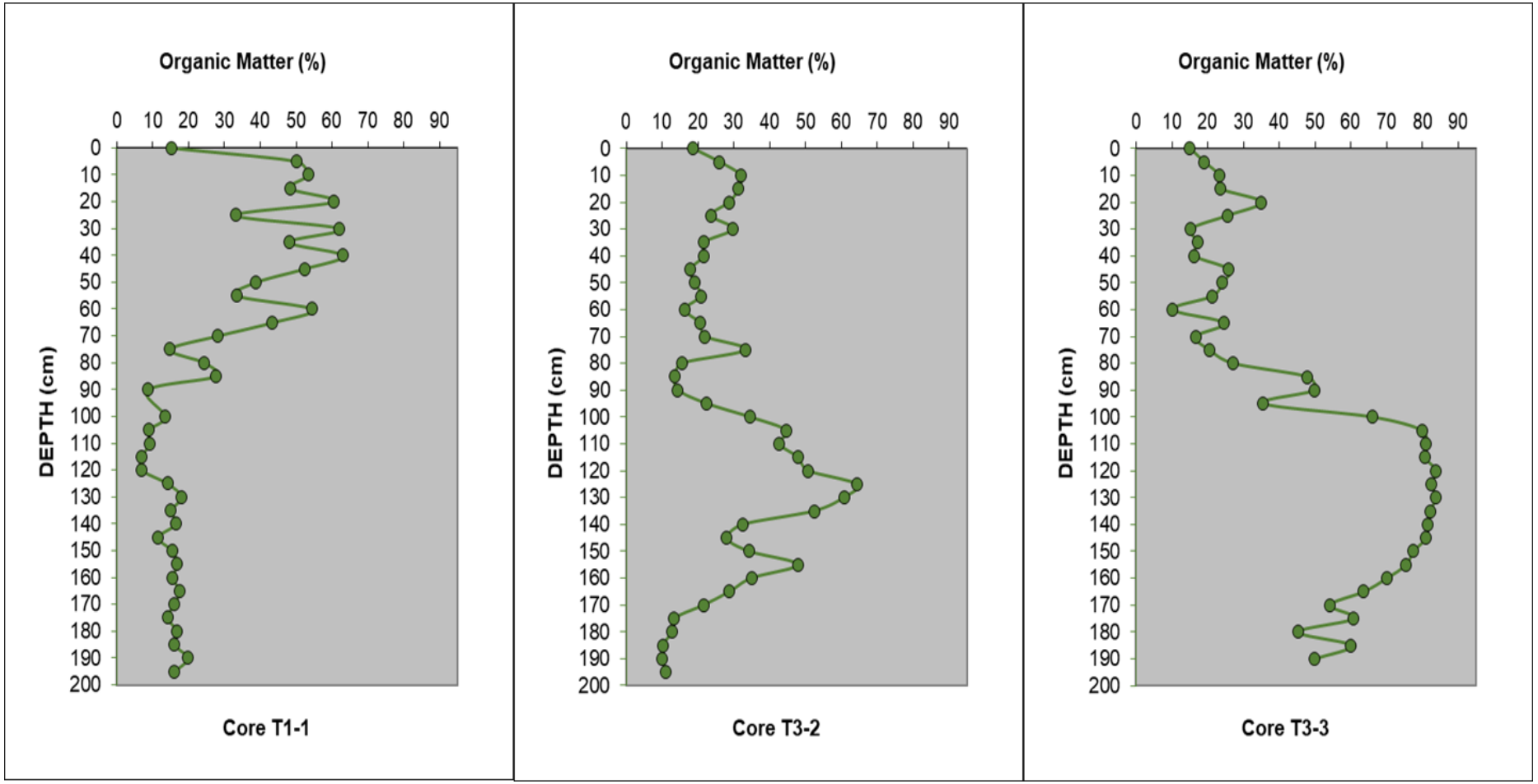

Figure S8 – Organic matter profiles from loss on ignition (LOI) for the upper 2 m of cores for representative bay (left), paleochannel (middle), and marsh (right) environments. Note even in bay environments, organic rich material is found immediately at depth for ~1 m. Paleochannel deposits are marsh environments that overlie paleochannels at depth (sometimes >2 m).

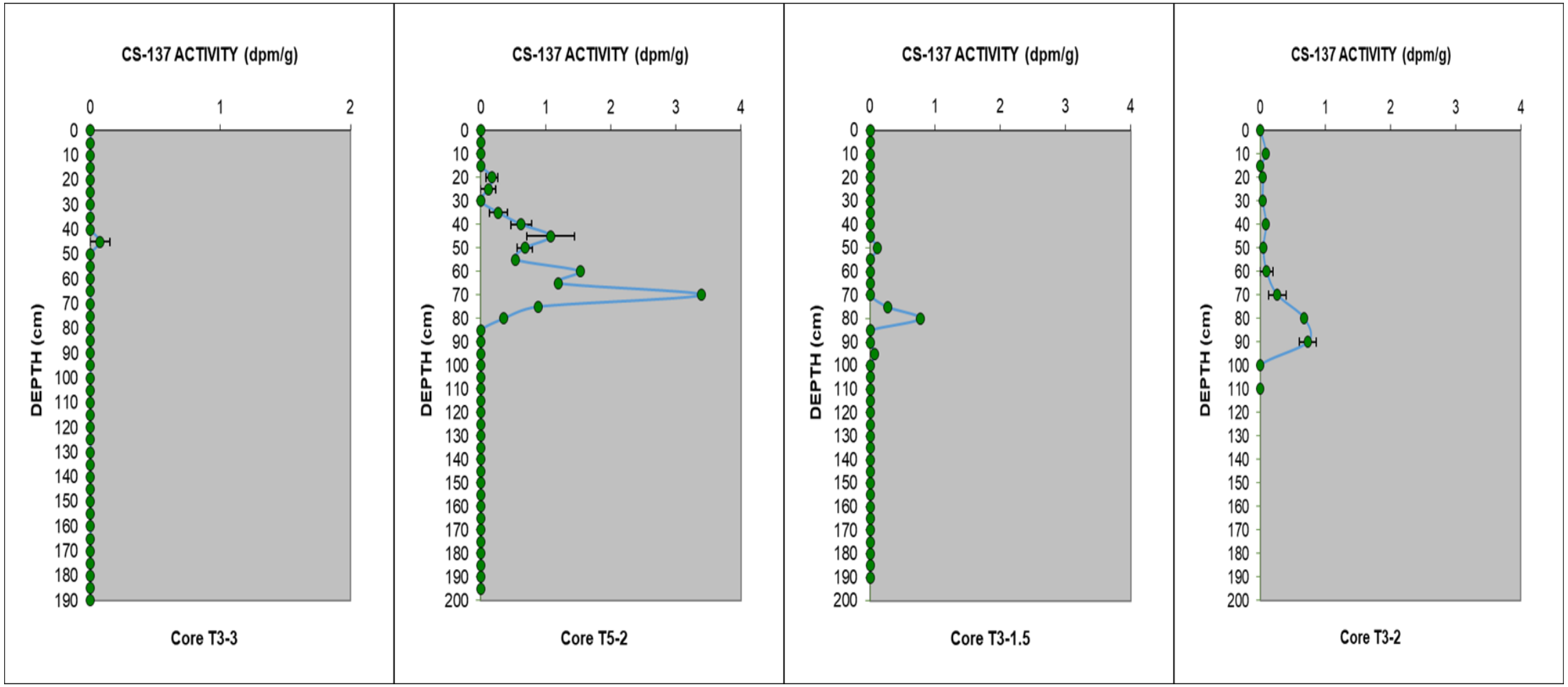

Figure S9 – Profiles of ^{137}Cs activity with depth. Peak downcore activity is indicative of the calendar year 1963. Note some cores display very obvious ^{137}Cs peaks, while others do not (T3-3).

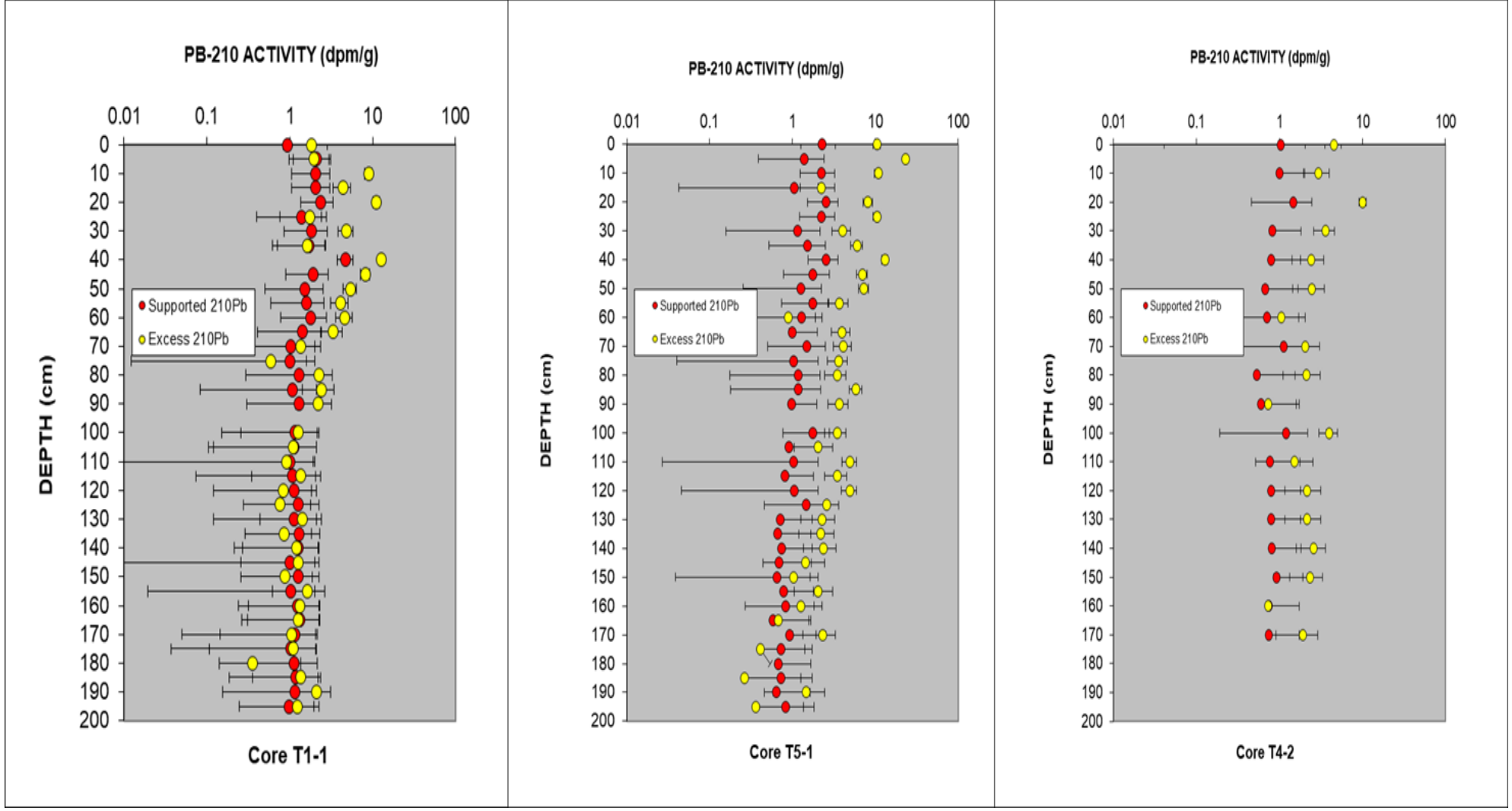

Figure S10 – Profiles of ^{210}Pb activity with depth for bay environment cores (where ^{137}Cs activity is not present). Linear regression of the excess activity provides vertical accretion rates over the past ~100 years.

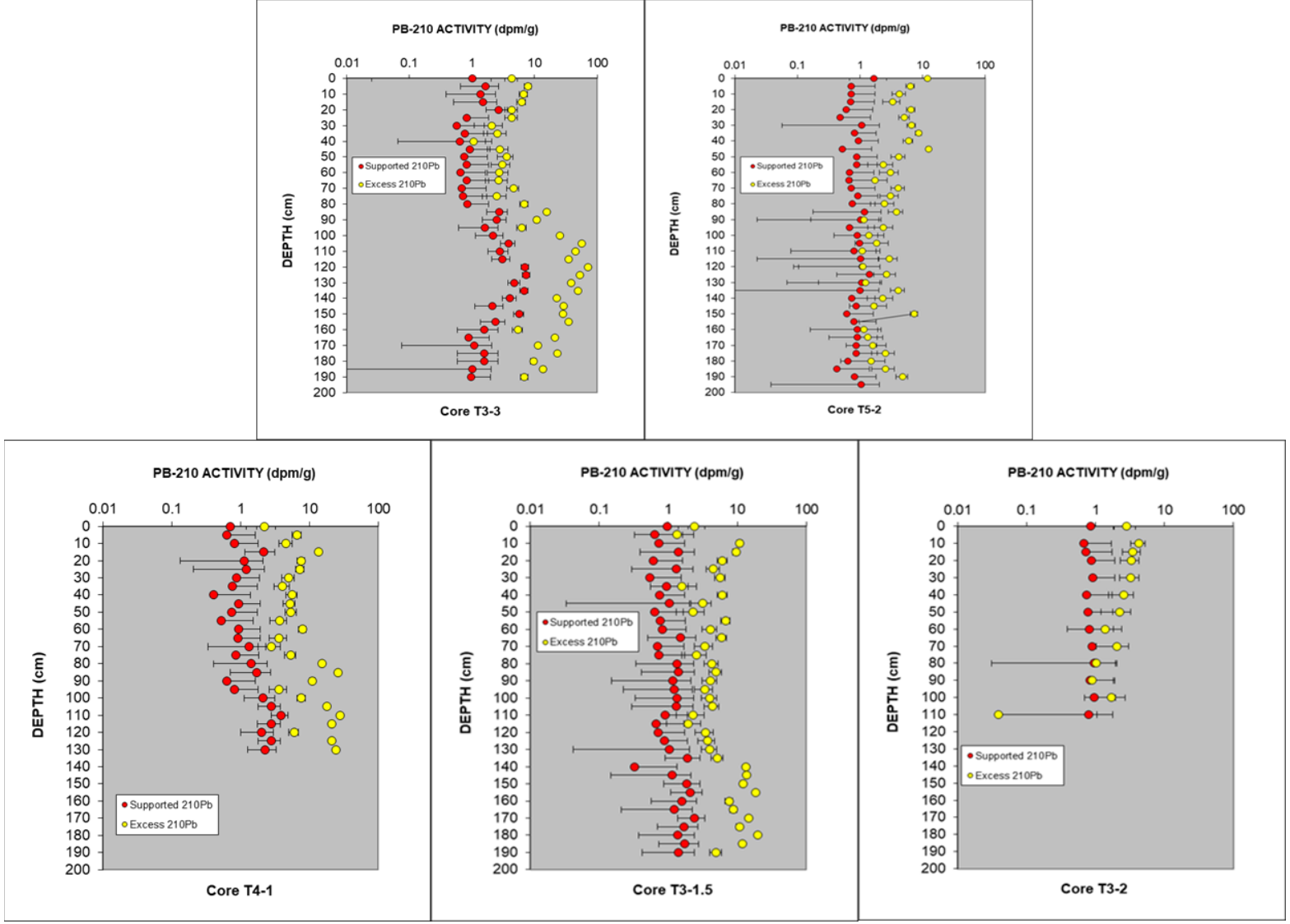

Figure S11 – Profiles of ^{210}Pb activity with depth for marsh (top) and paleochannel environment (bottom) cores. Paleochannel deposits are marsh environments that overlie paleochannels at depth (sometimes >2 m).

Figure S12 (this has been revised) – Long-term vertical accretion rates (VAR) across the Mid-Barataria Diversion Receiving Basin using 137Cs and 210Pb. Blue dots = Bay sites, purple dots = marsh/paleochannel sites. Includes cores from this study, Hughes (2016), Shrull (2018), and Vincent (2022). Note the lowest VARs from this study are from bay cores. See Piorkowski MS Thesis for explanation and interpretation.

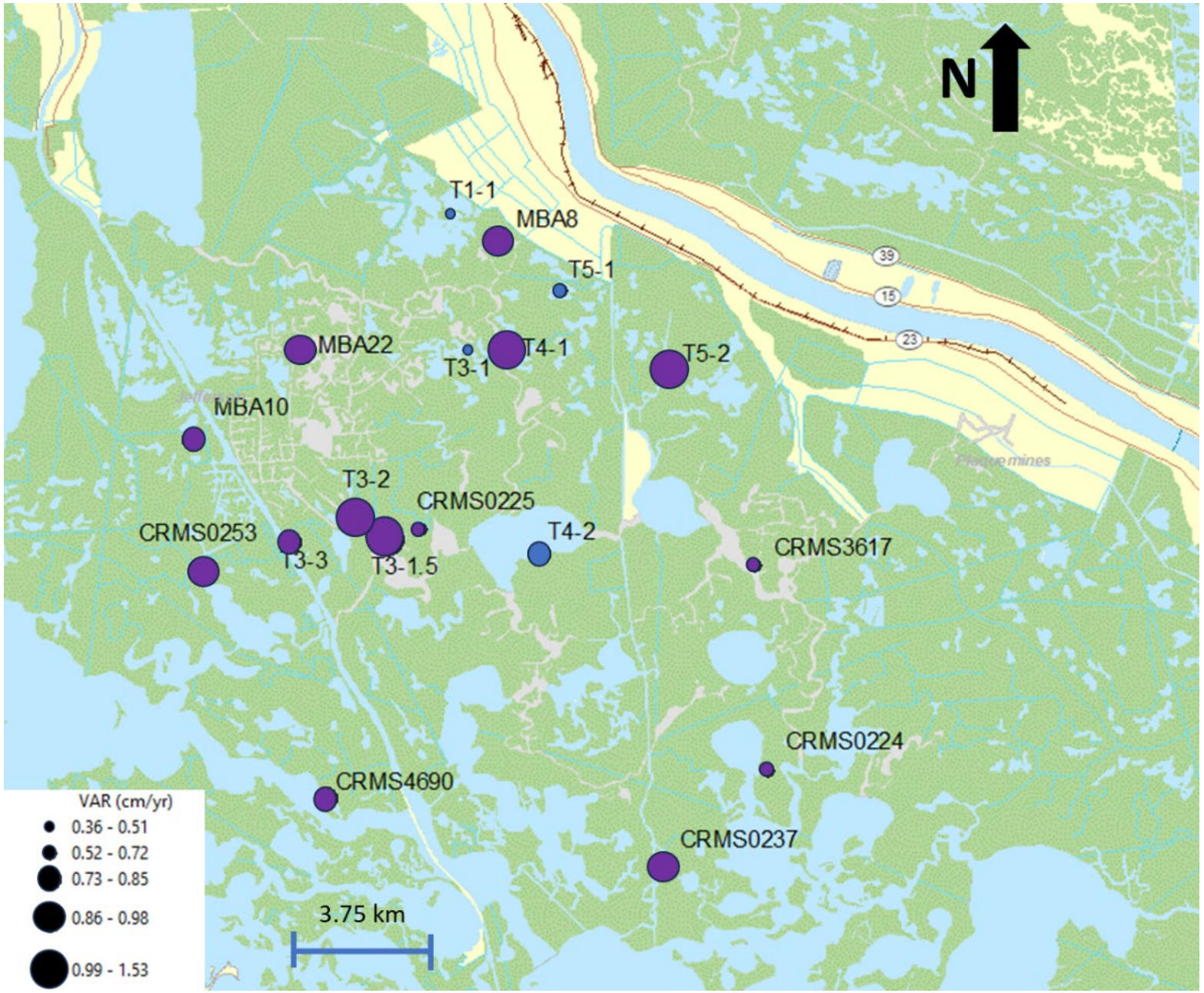

Figure S13 (this has been revised) – Age-depth plot from radiocarbon results from this study. These results give an indication of the Relative sea-level rise that has impacted the basin over the past ~3,000 years, however these are intercalated peat and organic samples (see Table S3), thus could also have been displaced vertically from overburden.

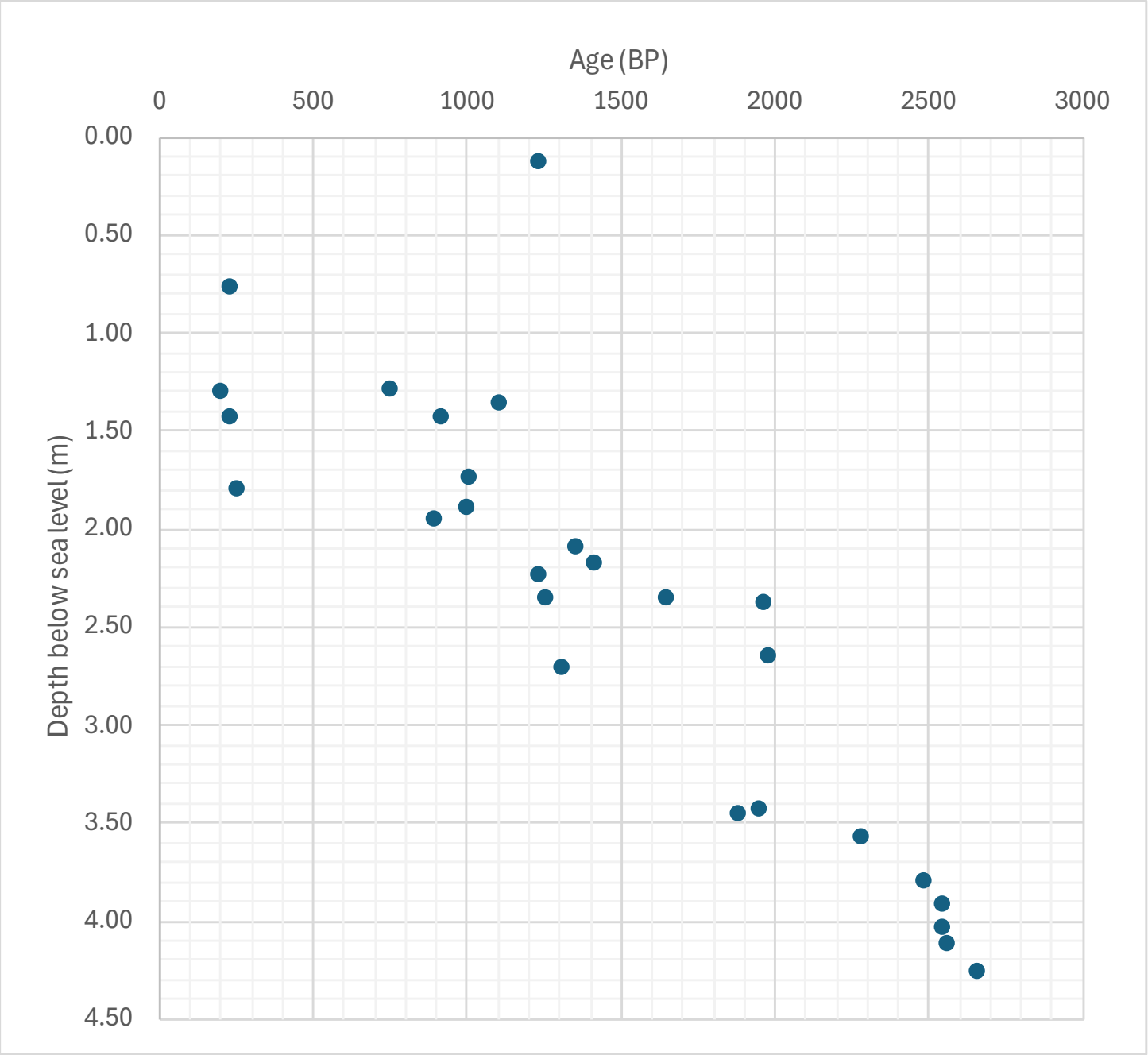
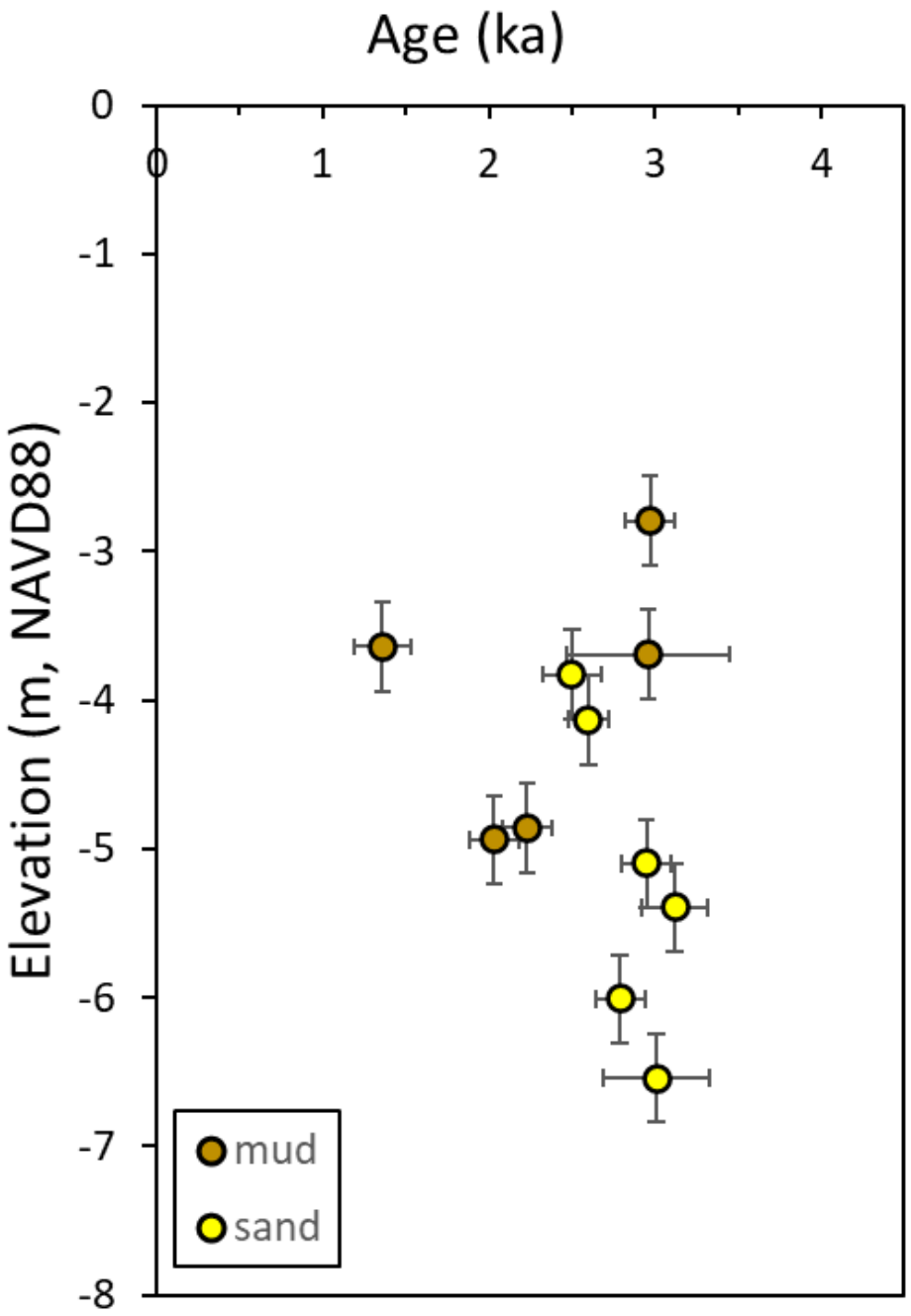
Figure S14 (this has been revised) – Age-depth plot from OSL results from this study. These results provide an indication of the Relative sea-level rise that has impacted the basin over the past ~3,000 years, however these results are not necessarily paleo sea-level indicators, as they could have been deposited as channel mouth bars (near or below coeval sea-level), channel infill (sub- to supra-tidal), or from crevasse splay deposits (sub-to supra-tidal).